Appl. Phys. B 72, 711–716 (2001) / Digital Object Identifier (DOI) 10.1007/s003400100580

Applied Physics B
Lasers
and Optics

High diffraction efficiency in SBN with applied fields near the coercive field

S.S. Sarvestani[1], **A. Siahmakoun**[1,*], **G. Duree**[1], **K. Johnson**[2]

[1] Department of Physics and Applied Optics, Rose-Hulman Institute of Technology, Terre Haute, IN 47803, USA
[2] Naval Surface Warfare Center, Crane Division, Crane, IN 47522, USA

Received: 6 December 2000/Revised version: 13 February 2001/Published online: 27 April 2001 –

Abstract. We present the experiments and results of our investigation of electrical fixing in SBN:60. We propose an optical method for determining the value of the coercive field in ferroelectric crystals. An interferometric method is used to map the change in the index of refraction with negative applied fields, where the minimum of the index change is an indication of the coercive field. From this experiment, values of $1.55\,\mathrm{kV} \pm 20\,\mathrm{V}$ for the coercive voltage and $147 \pm 6\,\mathrm{pm/V}$ for the linear electro-optic coefficient are found. Two electrical-fixing techniques that result in very high diffraction efficiencies are presented, discussed and compared to previous publications on electrical fixing in SBN. High diffraction efficiencies of about 95% were achieved with the application of negative fields near the coercive region, during and after holographic recording in the crystal.

PACS: 42.40.Ht; 42.70.Mp; 77.84.-s

Photorefractive materials have been used in numerous applications in many areas of optics, including image processing, real-time holography, optical information storage, and optical phase conjugation. Application of external fields has been found to enhance many of the desired properties of these materials, such as diffraction efficiency [1], photorefractive response time [2], and holographic storage capacity [3]. A detailed study of several electric-field-related effects in photorefractive crystals, such as amplitude and phase coupling, linear and nonlinear electro-optic effects, and the piezoelectric effect was conducted by De Vre et al. [4]. Hologram multiplexing has been demonstrated in photorefractive crystals with a variable electric field used to control the Bragg condition [5, 6].

In ferroelectric crystals in particular, externally applied electric fields have many interesting applications. Ding et al. studied the effect of the electric field history on the diffraction efficiency of ferroelectric KNSBN [7]. Photorefractive gratings are typically erased during the readout process, since the illumination by the readout beam causes a redistribution of charges in the crystal. In many applications of photorefractive materials, a fixed grating is required. Non-destructive readout is achieved by applying external electric fields to the crystal. Compared to the thermal-fixing technique [8–10], which is the most commonly used technique for fixing in photorefractive materials, electrical fixing offers the advantage of being a much faster and simpler procedure. The first group to report fixing by means of ferroelectric polarization and domain reversal was Micheron et al. [11]. In their experiment, an electric field, in the opposite direction to the spontaneous polarization, was applied after the grating was recorded. The same authors conducted a study [12] on the parameters of the fixing technique, where they found the minimum external field necessary to electrically fix a grating to be near the average coercive field, and the minimum time that the field must be applied to be the polarization switching time. Variations of this procedure include applying the depoling voltage during recording of the photorefractive grating [13, 14] and prior to the recording [15]. The formation and decay kinetics of ferroelectric domain gratings in SBN have been studied by Kewitsch et al. [16]. Electrical fixing has also been achieved for a large number of multiplexed holograms [17]. Recently, domain reversal was employed in bit-oriented three-dimensional optical memories [18].

During the course of our investigation on electrical-fixing techniques in $Sr_{0.60}Ba_{0.40}Nb_2O_6$, we were able to achieve extremely high diffraction efficiencies by means of various degrees of depoling during the exposure time. In this paper we report the results of our investigations on achieving high diffraction efficiencies with the aid of an applied electric field in an SBN:60 sample. We also present a novel way of achieving near-optical quenching in SBN by varying the amplitude of the applied electric field. We will begin by presenting a simple interferometric technique for determining the coercive field of a ferroelectric crystal. From the data obtained during this experiment we were able to calculate a reasonable value for the electro-optic coefficient, which validates our experimental results.

*Corresponding author.
(Fax: +1-812/877-8023, E-mail: azad.siahmakoun@rose-hulman.edu)

1 Coercive field measurement

The knowledge of the coercive field value is necessary in many applications of ferroelectric crystals such as electrical fixing, photorefractive switching, and photorefractive focusing and defocusing. In our experiment, the coercive field value must be known in order to achieve the highest value of diffraction efficiency and optical quenching. With external fields larger than the coercive field there is a decrease in the diffraction efficiency since depoling the crystal results in a smaller value for the electro-optic coefficient [14]. The coercive field is defined as the external field required to reduce the net polarization of the crystal to zero. The common method of finding this parameter is to map the hysteresis loop of the ferroelectric crystal by using the well-known Sawyer–Tower circuit [19]. This technique involves a low-frequency, high-voltage ac source and a high-voltage capacitor. Kahmann et al. [20] use beam-coupling topography to obtain spatially resolved hysteresis loops at room temperature. We propose an alternative optical method, which greatly reduces the level of difficulty. The experimental procedure is described in the following section and the theoretical considerations are presented following the procedure section.

1.1 Experiment

The crystal used in this experiment is a 6.2 mm × 6.2 mm × 5.2 mm SBN:60 with its *c*-axis along the [001] direction. Silver epoxy electrodes are applied to the crystal surfaces that are perpendicular to the *c*-axis and are used to apply dc voltage to the crystal and provide a means to monitor the current. An applied field is considered positive (negative) if it is in the direction (opposite) of the initial poling field. The technique proposed in this paper utilizes the front and back crystal surfaces to form a Fabry–Pérot interferometer, as shown in Fig. 1. An extraordinary-polarized He-Ne beam is incident on the crystal. The reflections from the front and the back surfaces of the crystal form an interference pattern comprised of concentric circles. The interference pattern is extracted from the incident beam path by means of a beam splitter. A 3× beam expander is used after the beam splitter to enlarge the fringe pattern to facilitate the isolation of a single fringe. To record and monitor the fringe shifts, a screen with a small hole is placed before a high-speed PIN detector such that a small portion of the central fringe is incident upon the detector. Application of a negative field causes an increase in the index of refraction due to the electro-optic effect, which results in a movement of the fringes toward the center of the pattern. By increasing the amplitude of the negative field slowly and continuously, we reach a critical point where the inward motion of the fringes stops and then changes direction to an outward motion. The value of the electric field applied at this turning point, where the motion of the fringes changes direction, is the value of the coercive field. This transition is also viewed on a CCD camera capturing the effect displayed on the screen.

In our experiment a triangular pulse with a slope of 20 V/s and amplitude of 1.9 kV is applied to the crystal in the negative direction. The signal from the detector is monitored on a digital oscilloscope. A typical detector signal along with the corresponding applied voltage pulse is shown in Fig. 2. The data gathered from this part of the experiment resulted in an average value of 1.55 kV ± 20 V for the coercive voltage limit.

We conducted the same experimental procedure but with a positive voltage (up to 2 kV) and recorded the fringe shift data. Linear regression for this set of data gives the following relation between the number of fringes, m, and the applied field: $m = 0.00283\,(\mathrm{m/V}) \times \boldsymbol{E} - 0.191$. One is able to calculate the linear electro-optic coefficient by combining equations: $\Delta\varphi = 2m\pi = \frac{2\pi}{\lambda}\Delta L\Delta n$ and $\Delta n = -\frac{1}{2}n_e^3 r_{33}E$, where $\Delta\varphi$ is the phase shift, ΔL is the difference in path length (in this case, twice the length of the crystal), and Δn is the refractive index change. By neglecting the small constant coefficient in the above relation for the number of fringes (which can be attributed to the initial phase, $\frac{\varphi_0}{2\pi}$, due to thermal effects), we obtain a value of $r_{33} = 147 \pm 6\,\mathrm{pm/V}$ for the linear electro-optic coefficient of this sample, which seems reasonable compared to published values for SBN:60.

1.2 Analysis and discussion

In a ferroelectric crystal, the spontaneous electric polarization can be reversed by means of an externally applied electric

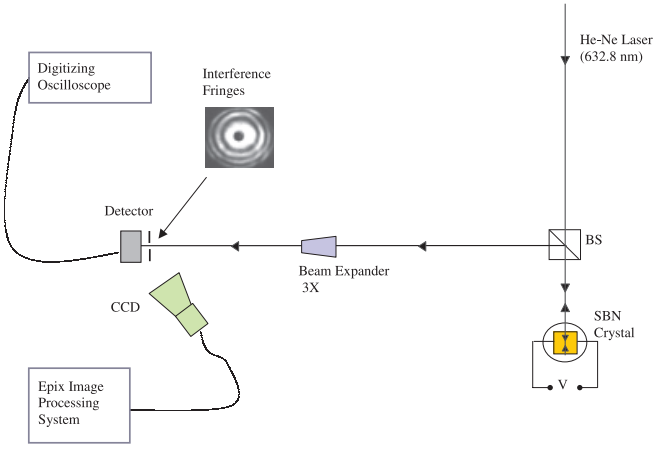

Fig. 1. Setup for coercive field measurement, front and back surfaces of crystal act as the Fabry–Pérot interferometer

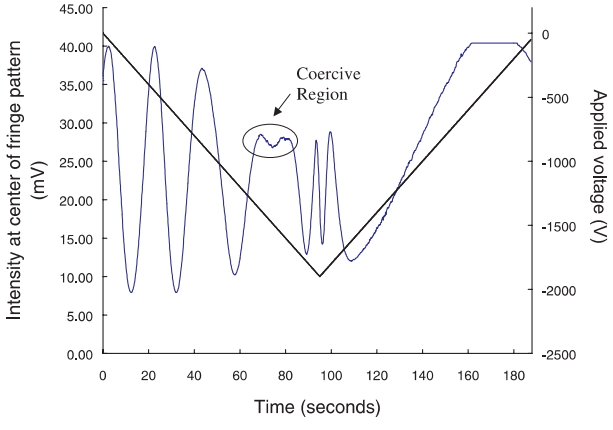

Fig. 2. Fabry–Pérot etalon fringe pattern movement during the application of a −1.9 kV triangular pulse

field. In the single-domain state of the crystal, all of the electric dipoles are aligned in the same direction. If an electric field is applied in the opposite direction, the orientation of the electric dipoles may reverse, depending on the strength of the dipole–dipole interaction and the interaction of the dipoles with the external field. As the amplitude of the electric field is increased, more and more dipoles will switch in the direction of the applied field. At the coercive field, an equal number of parallel and antiparallel domains exist in the crystal. In this experiment, we are only concerned with one branch of the hysteresis curve. In this region, the electric polarization in the material can be expressed as

$$P = \varepsilon_0 \chi E + a_1 \chi^{(2)} EE + a_2 \chi^{(3)} EEE + \dots , \quad (1)$$

where ε_0, a_1, a_2 are constants, χ is the electric susceptibility of the medium, and $\chi^{(2)}$,$\chi^{(3)}$ are higher-order tensors relating the polarization to the electric field. In terms of the impermeability tensor, this relationship may be written as

$$\eta_{ij}(E_{\text{ext}}) = \eta_{ij}(0) + \sum_k r_{ijk} E_k + \sum_k \sum_l s_{ijkl} E_k E_l + \dots , \quad (2)$$

where r_{ijk} is the linear electro-optic coefficient, and s_{ijkl} is the quadratic electro-optic coefficient. The change in index of refraction is expressed as

$$\Delta n_z = -\frac{1}{2} n^3 (r_{33} E_z + s E_z^2 + \dots), \quad (3)$$

where Δn_z represents the change in index of refraction along the c-axis, with respect to the applied electric field, r_{33} is the linear electro-optic coefficient, and s is the corresponding quadratic electro-optic coefficient. The minimum of this function denotes the value of the coercive field. A plot of the data obtained from the Fabry-Pérot interferometer and a corresponding second-order fit is shown in Fig. 3. However, a third-order fit is closer to the experimental data, which suggests that higher order electro-optic effects are present.

We believe that neither the linear nor the quadratic electro-optic effect is sufficient to explain the asymmetry in the detected fringe shifts around the coercive field. This observation in conjunction with the reduced number of whole fringe shifts as the voltage is gradually returned to zero suggests that depoling the crystal by application of negative field decreases the electro-optic coefficient [14]. The asymmetry in the curve in Fig. 2 after reaching the coercive field implies that a change has occurred in the material that affects the change in the index of refraction as a function of the applied field. Whereas, application of positive voltages does not alter the electro-optic coefficient since the crystal is initially single domain and remains in the saturation regime.

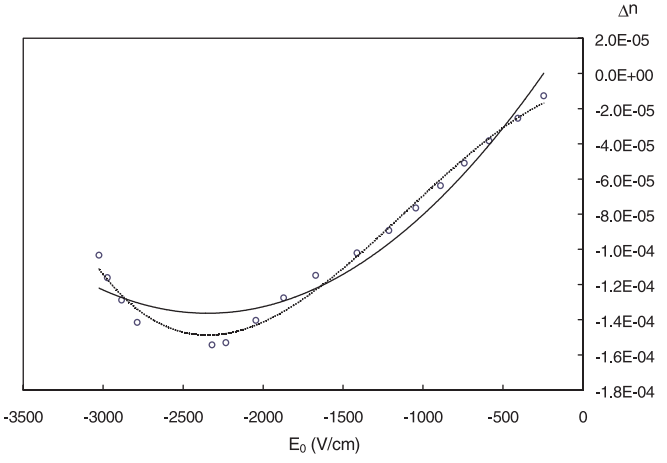

Fig. 3. Experimental plot of refractive index change versus applied electric field. Second- and third-order fits are shown with the *solid* and *dotted lines*, respectively

2 Constant and variable depoling fields

In this section we discuss the results of our investigation of electrical-fixing techniques in SBN:60. The procedure followed is close to the procedures reported in [13, 14]. This process is described as follows. A photorefractive grating is recorded in a single-domain crystal while simultaneously depoling with a negative applied field. After the recording beams are blocked and the voltage is removed, the crystal is illuminated by a non-Bragg-matched erasing beam. Upon the application of a positive pulse, a compensating space-charge grating is revealed. In our experiment, the depoling field is left on after the writing beams are blocked. Also, by varying the slope of the applied field during recording we obtain near-quenching efficiency in the SBN crystal. The experiment is described in the following section.

2.1 Constant depoling field

Two ordinarily polarized argon beams (514 nm) are used in the transmission geometry to record a grating with a grating spacing of $\Lambda = 9.9\,\mu$m, and grating vector parallel to the c-axis. The writing beams are expanded such that they fill the crystal to reduce the screening of the applied field by photoexcited charges. A low-intensity He-Ne beam is used to monitor the diffraction efficiency of the grating. A schematic of the setup is shown in Fig. 4. During our investigation we followed two different procedures for electrical fixing, both of which have resulted in remarkably high diffraction efficiencies. The two procedures differ in the amplitude and duration of the applied field. In the first procedure a negative voltage, -1.4 kV (less than the coercive voltage), is applied to the crystal followed by a short exposure (10 s) of the writing beams. After the negative voltage is removed (40 s), the diffraction efficiency is typically higher than 80%, whereas the diffraction efficiency of a grating written in the absence of applied field is 10 –15%. The diffracted beam intensity increases until it reaches a saturation level where it starts to decrease with a decay rate on the order of the He-Ne erasure. The crystal is then illuminated with an expanded, non-Bragg-matched, argon erasing beam. Upon the application of a repoling pulse (+3 kV for 2 s), a portion of the original space-charge field is revealed. The amplitude of this revealed grating is proportional to the positive applied field and is not observed when smaller depoling fields are applied. Figure 5 represents typical data obtained by this procedure. After each experiment is performed, the crystal must be carefully repoled. This often requires more than one repoling pulse, since

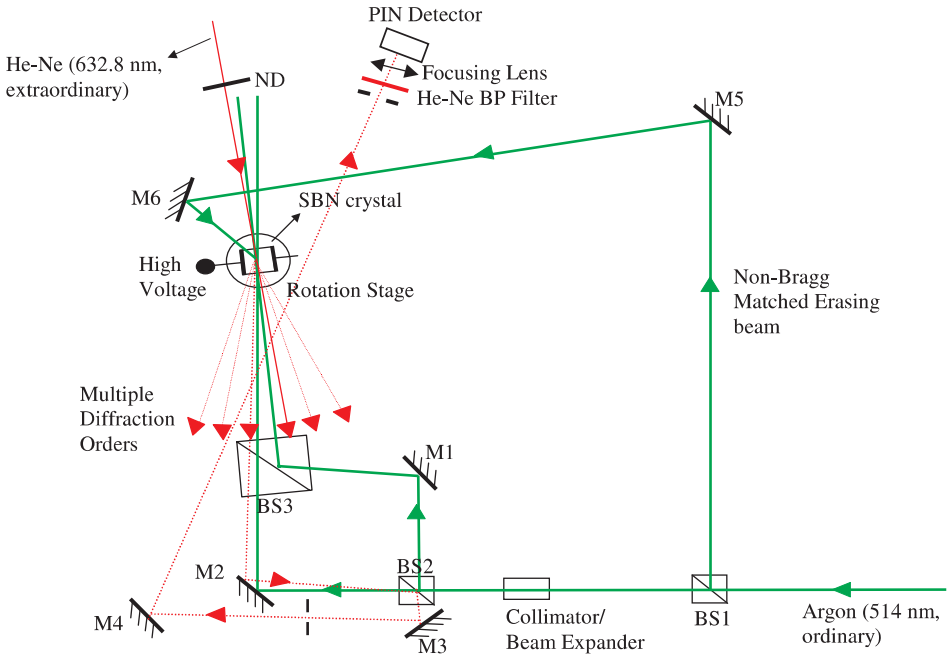

Fig. 4. Experimental setup for electrical fixing. Mirrors M1, M2 are used to guide the writing beams, while M2, M3, and M4 are used to direct the diffracted beam into the PIN detector

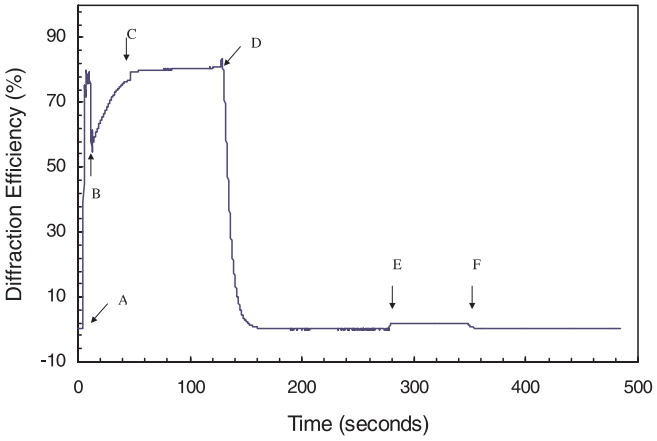

Fig. 5. Application of constant negative voltage during exposure. A –1.4 kV applied and writing beams exposed. B Writing beams blocked. C Voltage off. D Argon erasure. E Repoling pulse applied (+3 kV, 2 s). F Argon erasure

the space-charge field in certain regions reduces the net field, preventing the dipoles from switching back. To monitor the degree of repoling, an ammeter is inserted in series with the crystal to determine the switching current. When the switching current is reduced to zero, all the domains are aligned in the initial direction and the crystal is single domain [19].

The common explanation for electrical fixing in ferroelectric crystals is as follows. The process is qualitatively depicted by Fig. 6. Illuminating a single-domain crystal (Fig. 6a) with two coherent beams results in the formation of a space-charge field (E_{sc}) in the material (Fig. 6b). When the space-charge field is biased with an externally applied field (E_0) in the opposite direction of the initial poling field, 180° domains are formed which create a bound charge grating. These areas start in regions of the crystal where the external field and the space-charge field combine to a value at or above the coercive field (Fig. 6c). This 'domain grating' cannot be optically erased. To reveal the portion of the initial space-charge field that was bound to the domain grating, a positive field must be applied to the crystal. The function of the positive (repoling) pulse is to re-align the domains in the original configuration, effectively erasing the domain grating (Fig. 6d). Note that in Fig. 6, E_p represents the electric field produced by the dipole moments, not the dipole moments themselves. Therefore, when an external field is applied to the crystal, the dipoles align along the *c*-axis, in the direction of the applied field. Whereas the electric field produced by these dipoles, is in the opposite direction.

In our experiment, several critical points of the fixing procedure require a more specific explanation. Referring to Fig. 5, starting at point A, a space-charge field is being formed under the influence of the external field. The amplitude of the external field gives rise to the enhancement of the space-charge field, until it reaches a peak, at which point the domains start switching. The reversed domains cause a decrease in the diffraction efficiency because, as they form, some domains effectively cancel the effect of the space-charge field. After the writing beams are blocked (B), the space-charge field is fixed, whereas the dipole interaction continues. In this part of the process (B to C in Fig. 5), the domain grating is prevailing. This explanation is verified by the presence of a switching current in this region, as also observed by Cudney et al. [14] in regions where domains are switched. When the external field is removed (C), the modulation depth, which was reduced by the strong external field, is increased due to the linear electro-optic effect and results in a sudden increase in diffraction efficiency. After this point, the domains are stabilized, while there are domains present that are not bound to the space-charge [14]. Upon illumination with an erasing beam, the photoexcited charges move to compensate the free domains, which results in the initial rise in the diffraction efficiency. Erasing with a lower intensity beam, which results in a broader peak, confirms that this part of the process is of a photorefractive nature. After the initial rise, the erasing beam continues to redistribute the free

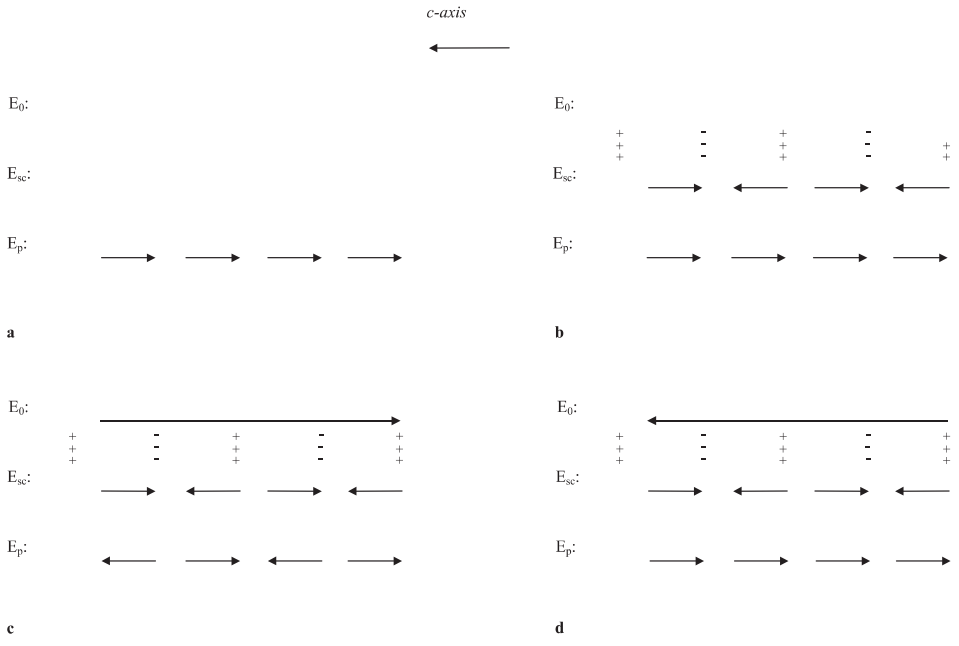

Fig. 6a–d. Principle of electrical fixing. **a** Single-domain crystal (E_p denotes the electric field produced by the dipole moments). **b** Induced space-charge field (E_{sc}). **c** Formation of domain grating with external field (E_0). **d** Application of positive field and return to single domain, while revealing compensating space-charge field

space-charge, until all the remaining charges are bound to the domains. Consequently, the diffraction efficiency steadily decreases until complete compensation is achieved, where no diffraction is observed. Finally, the positive voltage re-aligns the domains, revealing the remaining space-charge. It is possible to toggle between the previously bound portions of the domain grating and the photorefractive grating by successively applying negative and positive pulses.

2.2 Variable depoling field

In the second procedure a variable depoling field is applied to the crystal. Initially, −500 V is applied during the exposure time. After the diffraction efficiency reaches a stable saturation level, the amplitude of the negative voltage is increased. This results in a steady increase in the intensity of the diffracted beam until the external field reaches the coercive field value, beyond which, the diffraction efficiency starts to drop. This procedure differs with the previously described procedure in the fact that in this experiment, the space-charge field is actively involved in the formation of the gratings. In the ideal case (good phase stability between the writing beams and absence of multiple orders), with an external field slightly less than the coercive field, optical quenching can be achieved by means of complete depletion of the transmitted beam. Following this procedure we were able to observe diffraction efficiencies greater than 95%. The reproducibility of this experiment largely depends on the phase stability of the laser. As the phase changes, the grating is shifted and the readout fluctuates according to the instantaneous phase. A solution to this problem is to incorporate an active phase-stabilization system in the experiment. Without a phase-stabilization system we were able to increase the diffraction efficiency by a factor of 5 by repeating the procedure (alternating between applied voltage and exposure to writing beams). An example of this process is shown in Fig. 7. Another issue involved in our experiment is the multiple orders of diffraction present upon readout with a Bragg-matched He-Ne beam. We believe the presence of these orders is mainly due to the geometrical conditions of our experiment rather than the fringe-bending effect due to phase coupling as suggested in [4]. In our experiment the writing beams are ordinarily polarized which minimizes phase coupling. Also, the multiple orders are present even when a grating is recorded in the absence of an externally applied field. The presence of multiple gratings sets a maximum limit to the diffraction efficiency obtained in the first-order diffracted beam since even in the case of a completely quenched transmitted beam, the energy is distributed between the multiple orders.

In our experiment, five distinct diffracted orders are observed upon readout. The orders are situated as depicted in Fig. 4. By rotating the crystal by roughly 2 degrees we are able to tune in to each of the individual gratings. The presence of multiple orders indicates that the grating vector $\boldsymbol{K}_g$ is

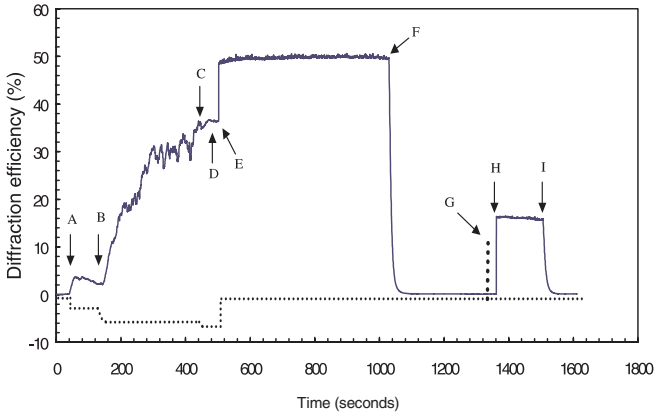

Fig. 7. Variable depoling field procedure (*dotted line* shows applied field). A −500 V and writing beams exposed. B Voltage decreased to −1.3 kV. C Voltage decreased to −1.4 kV. D Voltage off. E Writing beams blocked. F Argon erasure. G Repoling pulse in the dark (probe beam off). H Probe beam on. I Argon erasure

not uniquely defined. The angular spread of the grating vector in the case of this experiment is due to the curvature of the front surface of the crystal. This is also attributed to the observation of circular fringes in the Fabry–Pérot etalon experiment as shown in Fig. 1. The radius of curvature of the crystal surface is estimated to be -114.5 ± 10 cm. Therefore, a plane wave incident on the crystal is converged upon its entrance in the crystal. The converging interfering beams lead to angular distribution of the grating vector. When a Bragg-matched readout beam is incident on the crystal, the Bragg condition is satisfied for more than one grating vector, and multiple diffracted orders are observed.

3 Conclusions

We have demonstrated our findings on two field-enhanced recording procedures in photorefractive, ferroelectric SBN:60. The first experiment is similar to previously reported investigations on electrical fixing in SBN:75 by Qiao et al. [13], however, in our experiment we were able to achieve much higher diffraction efficiencies during the application of the negative voltage. In the experiment reported by Qiao et al., the diffraction efficiency of the recorded grating is of the same order both when a depoling field is applied after the grating is recorded and during the recording. In our experiment, the diffraction efficiency is increased by roughly a factor of 8, when a negative voltage is applied during the exposure time. This enhancement remains even after the voltage is removed. Also, in our experiment, the external field is left on after the writing beams are blocked, which results in a further enhancement of the diffraction efficiency by increasing the number of switched domains.

We presented a novel method for optical quenching. This method involves several considerations, which were discussed in this paper. An optical solution for the coercive field measurement was suggested, which also leads to a simple method for calculating the electro-optic coefficient.

Acknowledgements. The authors would like to thank the Office of Naval Research (ONR) and Dr. Dan Purdy for their support of this project under Contract No. N00014-00-1-0782.

References

1. J.P. Wilde, L. Hesselnik: Opt. Lett. **17**, 853 (1992)
2. K. Sayano, A. Yariv, R.R. Neurgaonkar: Opt. Lett. **15**, 9 (1990)
3. J.E. Ford, J. Ma, Y. Fainman, S.H. Lee, Y. Taketomi, D. Bize, R.R. Neurgaonkar: J. Opt. Soc. Am. A **9**, 1183 (1992)
4. R. De Vre, M. Jeganathan, J.P. Wilde, L. Hesselnik: J. Opt. Soc. Am. B **12**, 600 (1995)
5. A. Kewitsch, M. Segev, A. Yariv, R.R. Neurgaonkar: Opt. Lett. **18**, 534 (1993)
6. A.V. Chamrai, M.P. Petrov, V.M. Petrov: OSA Trends in optics and photonics series **27**, 515 (1999)
7. M. Ding, C.M. Cartwright, H. Zhang, W.A. Gillespie: OSA TOPS **27**, 380 (1999)
8. K. Buse, S. Breer, K. Peithmann, S. Kapphan, M. Gao, E. Kraetzig: Phys. Rev. B **56**, 1225 (1997)
9. B. Liu, L. Liu, L. Xu: Appl. Opt. **37**, 2170 (1998)
10. C.R. Hsieh, S.H. Lin, K.Y. Hsu, T.C. Hsieh, A. Chiou, J. Hong: Appl. Opt. **38**, 6141 (1999)
11. F. Micheron, G. Bismuth: Appl. Phys. Lett. **20**, 79 (1972)
12. F. Micheron, G. Bismuth: Appl. Phys. Lett. **23**, 71 (1973)
13. Y. Qiao, S. Orlov, D. Psaltis: Opt. Lett. **18**, 1004 (1993)
14. R.S. Cudney, J. Fousek, M Zgonik, P. Gunter: Appl. Phys. Lett. **63**, 3399 (1993)
15. R.S. Cudney, J. Fousek, M Zgonik, P. Gunter: Phys. Rev. Lett. **24**, 3883 (1994)
16. A. Kewitsch, M. Segev, A. Yariv, G. Salamo, T.W. Towe, E.J. Sharp, R.R. Neurgaonkar: Phys. Rev. Lett. **73**, 1174 (1994)
17. J. Ma, T. Chang, J. Hong, R. Neurgaonkar, G. Barbastathis, D. Psaltis: Opt. Lett. **22**, 1116 (1997)
18. M. Hisaka, H. Ishitobi, S. Kawata: J. Opt. Soc. Am. B **17**, 422 (2000)
19. F. Jona, G. Shirane: *Ferroelectric Crystals* (Pergamon Press, New York 1962)
20. F. Kahmann, R. Pankrath, R.A. Rupp: Opt. Commun. **107**, 6 (1994)